Carcinogenesis, 2021, Vol. 42, No. 5, 742–752

doi:10.1093/carcin/bgab016
Advance Access publication February 24, 2021
Original Article

ORIGINAL ARTICLE

RLIP depletion induces apoptosis associated with inhibition of JAK2/STAT3 signaling in melanoma cells

Sharad S.Singhal*, Atish Mohanty, Prakash Kulkarni, David Horne[1], Sanjay Awasthi[2] and Ravi Salgia

Department of Medical Oncology and [1]Department of Molecular Medicine, Beckman Research Institute, City of Hope Comprehensive Cancer Center and National Medical Center, Duarte, CA 91010, USA and [2]Department of Internal Medicine, Division of Hematology and Oncology, Texas Tech University Health Sciences Center, Lubbock, TX 79430, USA

*To whom correspondence should be addressed. Tel: +1 626 218 4238; Fax: +1 626 471 9374; Email: ssinghal@coh.org

Abstract

The incidence of malignant melanoma, a neoplasm of melanocytic cells, is increasing rapidly. The lymph nodes are often the first site of metastasis and can herald systemic dissemination, which is almost uniformly fatal. RLIP, a multi-specific ATP-dependent transporter that is over-expressed in several types of cancers, plays a central role in cancer cell resistance to radiation and chemotherapy. RLIP appears to be necessary for cancer cell survival because both *in vitro* cell culture and *in vivo* animal tumor studies show that the depletion or inhibition of RLIP causes selective toxicity to malignant cells. RLIP depletion/inhibition triggers apoptosis in cancer cells by inducing the accumulation of endogenously formed glutathione-conjugates. In our *in vivo* studies, we administered RLIP antibodies or antisense oligonucleotides to mice bearing subcutaneous xenografts of SKMEL2 and SKMEL5 melanoma cells and demonstrated that both treatments caused significant xenograft regression with no apparent toxic effects. Anti-RLIP antibodies and antisense, which respectively inhibit RLIP-mediated transport and deplete RLIP expression, showed similar tumor regressing activities, indicating that the inhibition of RLIP transport activity at the cell surface is sufficient to achieve anti-tumor activity. Furthermore, RLIP antisense treatment reduced levels of RLIP, pSTAT3, pJAK2, pSrc, Mcl-1 and Bcl2, as well as CDK4 and cyclin B1, and increased levels of Bax and phospho 5' AMP-activated protein kinase (pAMPK). These studies indicate that RLIP serves as a key effector in the survival of melanoma cells and is a valid target for cancer therapy. Overall, compounds that inhibit, deplete or downregulate RLIP will function as wide-spectrum agents to treat melanoma, independent of common signaling pathway mutations.

Introduction

Over the past decade, the incidence of cutaneous melanoma has risen faster than that of any other malignancy. Metastatic malignant melanoma affects about 9300 patients in the United States every year and almost inevitably leads to death. Melanoma presents with significant risk once it reaches the metastatic stage, due to its characteristic refractoriness to current modalities of chemotherapy (1–5). In addition to the exposure of melanocytes to UV radiation, loss of *CDK2NA* is a significant risk factor for melanomagenesis and accounts for 70% of genetically predisposed cases of melanoma. Current therapeutic drugs for advanced melanoma, including dacarbazine [objective response rate (ORR) ~18%], temozolomide (ORR ~15%), paclitaxel (ORR ~13%), cisplatin (ORR ~23%), docetaxel (ORR ~11%), lomustine (ORR ~13%) and carboplatin (ORR ~16%), offer only a partial benefit. Although combination treatments, such as dacarbazine with immune-boosting drugs like ipilimumab, have yielded higher 1-year survival rates (47.3%), they have also been found to reduce 3-year survival rates (20.8%) and increase the occurrence of grade 3–4 toxicities (56.3%), limiting their potential application in the clinic (1–3). In this context, there is a greater need for new candidate drugs capable of targeting multiple critical nodes of melanoma signaling. BRAF-targeted therapy has recently emerged as the most effective therapy for melanoma, but response rates are less than desirable, and the survival advantage is relatively short (4–6).

Received: January 29, 2021; **Revised:** February 14, 2021; **Accepted:** February 19, 2021

Abbreviations

ABC	ATP-binding cassette
CDE	clathrin-dependent endocytosis
DOX	doxorubicin
GS-E	glutathione-electrophile conjugate
GSH	glutathione
GST	glutathione-S-transferase
HAVSMC	human aorta vascular smooth muscle cells
HUVEC	human umbilical vascular endothelial cells
IOVs	inside-out vesicles
JAK2	Janus-activated kinase-2
MAP	mercapturic acid pathway
NHDF	normal human dermal fibroblast
ORR	objective response rate
PBS	phosphate-buffered saline
Pgp	P-glycoprotein
STAT3	signal transducer and activator of transcription 3
TUNEL	triphosphate nick-end labeling

Melanoma cells characteristically express high levels of transporter proteins in their membranes, which may contribute to both drug resistance and radiation resistance. Nevertheless, targeting the ATP-binding cassette (ABC) transporter family of proteins has not been effective in reversing drug-resistance in melanoma. Cell line, animal and human clinical data indicate that the ABC transporters MRP, P-glycoprotein (Pgp) and others can mediate drug accumulation defects in malignant cells; however, their correlations with pathology, clinical resistance and outcomes in melanoma are poor, and attempts to improve therapeutic efficacy by targeting them have not been successful (7,8). Although alternative targeting strategies may ultimately prove efficacious (9), inhibitors of ABC transporters have not yet been successful in clinically improving chemotherapeutic outcomes (8). These findings clearly indicate that other transport and resistance mechanisms are involved (10).

The current study aimed to supply and interrogate a missing piece of the puzzle: the multi-specific transporter RLIP. RLIP is a stress-responsive non-ABC, high-capacity transporter, which is likely to have had a significant confounding effect in the previous studies on ABC transporters in melanoma. Compared with normal cells, cancer cells appear significantly more sensitive to apoptosis triggered by blocking RLIP, suggesting the feasibility of targeting RLIP in melanoma therapy. In contrast, the genetic deletion of RLIP causes the loss of about 70% of total glutathione-electrophile conjugate (GS-E) transport activity, along with major phenotypic effects due to sensitivity to stress- and toxin-mediated apoptosis. The loss of GS-E transport activity results in the accumulation of GS-Es and their electrophilic precursors (e.g., GS-HNE and 4HNE) in animal tissues (11–14).

The mercapturic acid pathway (MAP) is known to be highly upregulated in melanoma, as demonstrated by several previous studies showing increased expression of glutathione (GSH), glutathione S-transferases (GSTs) and other GSH-linked enzymes (15). Melanoma cells are typically rich in MAP enzymes, as well as clathrin-dependent endocytosis (CDE). Both the MAP and CDE play crucial roles in antagonizing apoptosis, promoting tumor growth and invasion and resisting therapeutic interventions, such as chemotherapy, biological therapy and radiotherapy. We previously demonstrated that melanoma contains more RLIP protein per cell than any other cancer, and this expression level correlates with CDE of fluorescently labeled epidermal growth factor. We also showed that cultured mouse B16 melanoma cells are susceptible to RLIP blockade by antibodies and RLIP depletion by antisense oligonucleotides and siRNA; moreover, B16 melanoma subcutaneously implanted into C57Bl/6 mice undergoes sustained regression upon RLIP depletion or inhibition (16). Until now, we had not yet studied human melanoma cell lines or xenografts to determine whether the effects of RLIP depletion/inhibition in B16 cells represent a generalized phenomenon. Furthermore, we had not evaluated the role of RLIP in cell motility, invasiveness, CDE or other Ral-regulated movement pathways.

Thus, we sought to determine whether RLIP depletion/inhibition has broad-spectrum efficacy against human melanoma xenografts, regardless of genetic background, as we have demonstrated in mouse melanoma and other human neoplasia. Natural products or synthetic compounds inspired from natural products continue to be excellent sources for new drug candidates, especially in the area of anticancer therapeutic. We predicted that like spirooxindole derivatives (SOID-1 to SOID-12) and a small molecule 6-bromoindirubin-3′-oxime–mediated growth inhibition of human melanoma cells (17–19), RLIP depletion/inhibition would be accompanied by apoptosis, inhibition of CDE and blockade of JAK2/STAT3 signaling used by melanoma cells to avoid apoptosis and promote growth. CDE determines the strength of growth-factor induced mitogenic signaling and STAT3 activation (20). Therefore, the present studies were designed to examine the effects of inhibiting the transport activity of RLIP on melanoma cells in culture and tumor xenografts in nude mice, with a focus on developing a novel RLIP-targeted therapeutic strategy for the treatment of melanoma.

Materials and methods

Materials

The terminal deoxynucleotidyl-transferase deoxyuridine triphosphate nick-end labeling (TUNEL) fluorescence apoptosis kit and avidin/biotin complex detection kit were purchased from Promega (Madison, WI) and Vector (Burlingame, CA), respectively. MTT (3-(4, 5-dimethylthiazol-2-yl)-2, 5-diphenyltetrazolium bromide) was purchased from Sigma–Aldrich (St. Louis, MO). Antibodies for CD31, Ki67, cyclin B1, CDK4, Bcl2, Mcl-1, Bax, pJAK2 ($Tyr^{1007/1008}$), JAK2, pSTAT3 (Tyr^{705}), STAT3, pSrc (Tyr^{416}), Src, β-actin and phospho 5' AMP-activated protein kinase (pAMPK) (T^{172}) were purchased from Cell Signaling Technologies (Danvers, MA). RLIP antibodies were purchased from Santa Cruz Biotechnology (Columbus, OH). Anti-rabbit and anti-mouse horseradish peroxidase–conjugated secondary antibodies were purchased from Cell Signaling Technologies. Doxorubicin (DOX, Adriamycin) was obtained from Adria Laboratories (Columbus, OH). ^{14}C-DOX (specific activity 43.6 Ci/mmol) was purchased from NEN Life Sciences (Boston, MA). ^{3}H-GSH (3000 Ci/mmol) was purchased from Pharmacia Biotech (Piscataway, NJ). DNP-SG (2,4-dinitrophenyl-S-glutathione) was synthesized from CDNB (1-chloro-2,4-dinitrobenzene) and GSH according to the method described previously (21). The Universal Mycoplasma Detection Kit was procured from the American Type Culture Collection (ATCC; Manassas, VA).

Cell lines and cultures

Human melanoma cell lines (A2058, A375, G361, MeWo, A101D, SKMEL2, SKMEL5 and SLMEL28) were purchased from ATCC. Normal human dermal fibroblasts (NHDF) were kindly provided by Dr Jun Wu, Tumor Biology Core, City of Hope, Duarte, CA. Human aortic vascular smooth muscle cells (HAVSMC) and human umbilical vascular endothelial cells (HUVEC) were kindly provided by Dr Fiemu Nwariaku, University of Texas Southwestern Medical Center, Dallas, TX. All cells were cultured at 37°C in a humidified atmosphere of 5% CO_2 in the appropriate medium: RPMI 1640 (A2058, A375, G361, MeWo, SKMEL2, SKMEL5 and SKMEL28), DMEM (A101D, HAVSMC and NHDF) or EGM-2 BulletKit (HUVEC), supplemented with 10% (v/v) heat-inactivated FBS and 1% (v/v) penicillin/streptomycin (P/S). Cell

lines were authenticated by analyzing 15 different human short tandem repeats by the City of Hope Integrative Genomics Core, Duarte, CA. All cells were tested for *Mycoplasma* once every 3 months.

RLIP phosphorothioate antisense preparation

Chemically synthesized phosphorothioate DNA in desalted form was purchased from Biosynthesis, Inc (Lewisville, TX). A 21-nucleotide-long scrambled phosphorothioate DNA was used as a control (16).

MTT cell viability assay

MTT assays were used to determine the effects of RLIP inhibition and depletion on the viability of melanoma cells (A2058, A375, G361, MeWo, A101D, SKMEL2, SKMEL5 and SKMEL28) and normal cells (NHDF, HAVSMC and HUVEC). Cells were seeded in 96-well plates (5,000 cells/well) and treated for 48 h with RLIP IgG (40 μg/ml) or transfected with RLIP antisense (20 μg/ml) using Maxfect Transfection Reagent (MoleculA, Inc), according to the manufacturer's protocol. Next, 10 μl MTT (5 mg/ml) was added to each well, and the plates were incubated for 4 h at 37°C. Later, the medium was removed, and the cells were washed with phosphate-buffered saline (PBS). The resulting formazan crystals were dissolved in 100 μl of DMSO, and the absorbance reading of each well was taken at 570 nm using a plate reader (Microplate XMark™ spectrophotometer; Bio-Rad, Hercules, CA). The percentage of cell survival was determined based on the background-corrected absorbance, as shown in the following formula: cell survival (%) = ($Absorbance_{Treatment}$/$Absorbance_{Control}$) × 100. The data shown represent the mean and standard deviation of data from three independent experiments, each with eight replicate wells per treatment. Western blot analyses confirmed the extent of RLIP depletion using RLIP antisense.

Detection of RLIP protein expression in normal and melanoma cell lines

Melanoma cells (A2058, A375, G361, MeWo, A101D, SKMEL2, SKMEL5 and SKMEL28) and normal cells (NHDF and HUVEC) were collected by trypsinization, washed with PBS and then lysed using sodium dodecyl sulfate lysis buffer (Cell Signaling Technologies) containing protease and phosphatase inhibitors (Roche, Indianapolis, IN). The cell pellets were briefly sonicated to dissociate cell membranes. Fifty microgram of total protein isolated from these cells was electrophoresed on 12.5% sodium dodecyl sulfate–polyacrylamide gels at 200 V for 1 h and then the proteins were then transferred to nitrocellulose membranes at 100 V for 70 min at 4°C. The blots were then probed with primary antibodies against RLIP (1:1000) overnight at 4°C. The next day, the blots were rinsed with 1× TBS-tween (0.1%) and probed with horseradish peroxidase–conjugated secondary antibodies (1:5000) for 1 h at room temperature. The blots were analyzed using SuperSignal West Pico Chemiluminescent Substrate (Thermo Fisher Scientific, Rockford, IL), and images were captured using a MultiImage Light Cabinet (Alpha Innotech, San Leandro, CA). RLIP protein expression levels were normalized to β-actin expression levels. Western blot analysis was performed in triplicate, and images shown represent typical replicates.

TUNEL assays to detect the effects of anti-RLIP IgG on apoptosis

To measure apoptosis, DNA fragments were labeled by TUNEL and detected using a Promega Apoptosis Detection Kit, according to the manufacturer's protocol. Briefly, aliquots of cells (1×10^5) were plated on coverslips in 12-well plates and incubated for ~12 h, followed by treatment with either pre-immune serum or anti-RLIP IgG (40 μg/ml final concentration). After 24 h, the cells were washed with PBS. Apoptotic cells were detected by green fluorescence and characteristic shrinkage.

Transport studies in inside-out vesicles

Crude membrane inside-out vesicles (IOVs) were prepared from the normal cells (NHDF, HAVSMC and HUVEC) and melanoma cells (A2058, A375, G361, MeWo, A101D, SKMEL2, SKMEL5 and SKMEL28) using procedures that we previously established for K562 human erythroleukemia cells (11,22). The transport of DOX and DNP-SG by IOVs was evaluated using the method previously described (11). The ATP-dependent uptake of ^{14}C-DOX was determined by subtracting the radioactivity (cpm) of the control IOVs (without ATP) from that of the experimental IOVs containing ATP; the transport of DOX was calculated in terms of pmol/min/mg IOV protein. The transport of ^{3}H-DNP-SG was measured in a similar manner. Each determination was performed in triplicate.

Transport studies in IOVs coated with antibodies

IOVs (20 μg protein/30 μl reaction mixture) were incubated with 1 μg of anti-RLIP, anti-MRP1 or anti-Pgp antibodies for 30 min at room temperature. In one control reaction, IgG was excluded, and in the other control, IOVs were incubated with pre-immune IgG. After incubation, the ATP-dependent transport of ^{14}C-DOX in the antibody-coated vesicles was measured.

In vivo xenograft studies

All animal experiments were carried out according to a protocol approved by the City of Hope Institutional Animal Care and Use Committee. Hsd:Athymic nude (*nu/nu*) mice were obtained from Charles River (Wilmington, MA) and acclimated to the facility for 1 week before the beginning of the experiment. After acclimation, twenty 8-week-old mice were subcutaneously injected in one flank with 1×10^6 SKMEL2 cells suspended in 100 μl of PBS. At the same time, the animals were randomly divided into four groups ($n = 5$) for treatment with pre-immune serum, RLIP antibodies, control scrambled antisense or RLIP antisense (5 mg/kg b.w. each). Treatment was started 10 days after SKMEL2 cell implantation, once tumor growth was palpable. Treatments were administered via intraperitoneal injection once a week for 7 weeks. A similar protocol was followed for SKMEL5 xenografts studies. Animals were examined daily for signs of tumor growth. Tumors were measured in two dimensions using calipers, and body weights were recorded. Photographs of the animals were taken on days 1, 10, 20, 30, 40 and 50 after the initiation of treatment. Photographs of the tumors were also taken on day 50. At the end of the study, the mice were euthanized by CO_2 asphyxiation, followed by cervical dislocation. Tumor weights were compared between groups using an unpaired Student's *t*-test. Tumors were fixed in 10% buffered formaldehyde solution and paraffin-embedded for immuno-staining or were snap-frozen in liquid nitrogen for further molecular analysis, such as western blot analysis.

Immunohistochemistry

Tumor tissues from mice in all four treatment groups (treated with pre-immune serum, RLIP antibodies, control scrambled antisense or RLIP antisense) were collected, fixed in buffered formalin for 24 h, embedded in paraffin, cut into 5 μm thick sections and mounted on poly-L-lysine–coated slides. Tissue sections were stained with hematoxylin and eosin, and antibodies against RLIP, Ki67, CD31 and pAMPK were detected using a universal avidin/biotin complex detection kit (Vector). Immunoreactive areas were marked by dark brown staining, whereas non-reactive areas displayed only background staining. Photomicrographs were acquired using an Olympus DP 72 microscope with ×40 magnification. The intensity of antigen staining was quantified by digital image analysis using DP2-BSW software.

Statistical analysis

Unless otherwise specified, data are presented as mean ± standard deviation for at least three independent experiments. Changes in tumor size and body weight during the course of the experiments were visualized by scatter plot. The statistical significance of differences between the control and treatment groups was determined by paired *t*-tests or two-way ANOVA. $P \leq 0.05$ was considered statistically significant.

Ethics statement

No human subjects were involved in the present study. All animal studies were conducted according to a protocol approved by the City of Hope Animal Care and Ethics Committee (IACUC protocol # 20033). Any mice showing signs of distress, pain or suffering due to tumor burden were humanely euthanized.

Results

Expression of RLIP

RLIP is a ubiquitously expressed protein that is most highly expressed during embryonic development. In adult life, it is found primarily in the vascular endothelium and kidney. Lower amounts are expressed in normal adult lung, pancreas, muscle and bone marrow (11–13). Genome-wide expression studies have revealed that, compared with normal parenchyma, cancer cells nearly uniformly overexpress RLIP. Increased RLIP protein levels have been reported in various cancer cell lines and tissues compared with their normal counterparts (16,23–25). Therefore, we investigated the expression of RLIP protein in various human normal cells (NHDF and HUVEC) and melanoma cells (A2058, A375, G361, MeWo, A101D, SKMEL2, SKMEL5 and SKMEL28). Western blot analyses of membrane protein extracts from these cells, performed against anti-RLIP IgG, indicated higher RLIP protein levels in melanoma versus normal cells (Figure 1A), which was confirmed by immunohistochemistry (Figure 1B). In addition, we found that RLIP protein levels were reduced in melanoma cells (SKMEL2 and SKMEL5) upon treatment with RLIP antisense (Figure 1C).

Inhibition of RLIP induces apoptosis

To assess the mechanisms underlying the cytotoxicity of RLIP inhibition, we measured apoptosis using immunohistochemical TUNEL assays. In TUNEL assays, the induction of apoptosis is visualized as green fluorescence. This assay did not reveal detectable apoptosis in the NHDF cells treated with pre-immune IgG or anti-RLIP IgG, or in the SKMEL2 or SKMEL5 melanoma cells treated with pre-immune serum; however, apoptosis was observed in the SKMEL2 and SKMEL5 melanoma cells treated with anti-RLIP IgG (Figure 1D). This suggests that RLIP may be an attractive target for inhibiting melanoma growth.

Table 1 shows RLIP protein concentrations and transport activity in melanoma and nonmalignant normal cell lines. The amount of total crude membrane protein obtained from 100 × 10^6 cells in log-phase growth were comparable for normal and cancer lines. RLIP represented 0.19 ± 0.02% and 0.83 ± 0.14% of the total detergent-soluble protein from the membranes of normal and melanoma cells, respectively (Table 1). These percentages of total membrane protein are within the range previously determined for other cell lines (16).

Transport activity of RLIP is greater in melanoma cells

We have shown that proteoliposomes reconstituted with RLIP mediate the ATP-dependent transport of DOX and other drugs (11,26). In order to examine whether the differential RLIP protein expression in normal and melanoma cells is reflected in their transport activity, we compared the ATP-dependent uptake of DOX and DNP-SG in crude membrane IOVs prepared from the membranes of control and melanoma cells. The results presented in Table 1 clearly demonstrate that IOVs prepared from melanoma cells had significantly higher ATP-dependent transport of DOX and DNP-SG than IOVs prepared

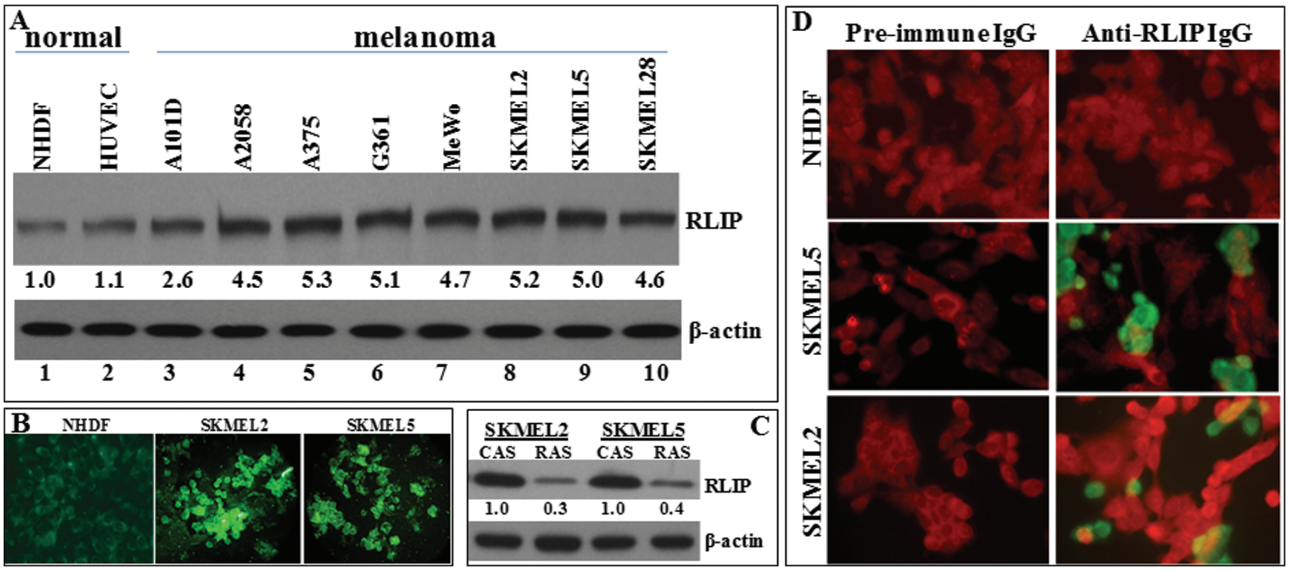

Figure 1. RLIP levels in normal versus melanoma cells. **(A)** Fifty microgram of protein from normal cells (NHDF and HUVEC) and melanoma cells (A101D, A2058, A375, G361, MeWo, SKMEL2, SKMEL5 and SKMEL28) was loaded onto 12.5% sodium dodecyl sulfate–polyacrylamide gels, electrophoresed, transferred to nitrocellulose membranes and probed with anti-RLIP IgG as the primary antibody and horseradish peroxidase–conjugated goat anti-rabbit IgG as the secondary antibody. β-Actin was used as a loading control. The experiment was performed three times, with one representative image shown here. **(B)** RLIP expression was also evaluated by the immunohistochemical analysis of melanoma (SKMEL2 and SKMEL5) and normal (NHDF) cell lines. For immunohistochemical localization studies, anti-RLIP IgG was used as the primary antibody and FITC-conjugated goat anti-rabbit IgG was used as the secondary antibody. **(C)** Western blot analysis was also conducted 24 h after treatment with scrambled control antisense (CAS) or RLIP antisense (RAS; 20 μg/ml final concentration) using Maxfect transfection reagent. Fifty microgram of protein was loaded onto the gels, and the blots were probed with anti-RLIP IgG. β-Actin was used as a loading control. The numbers below the blots represent the fold change in protein levels compared to the control, as determined by densitometry. The experiment was performed three times, with one representative image shown here. **(D)** Effect of anti-RLIP IgG on apoptosis, as determined by TUNEL assays. Melanoma (SKMEL2 and SKMEL5) and normal (NHDF) cells were grown on coverslips, treated with either pre-immune serum or anti-RLIP IgG (40 μg/ml final concentration) for 24 h and then washed with PBS. TUNEL assays were performed using the Promega Apoptosis Detection Kit and examined using a Zeiss LSM 510 META laser scanning fluorescence microscope with filters 520 and 620 nm. Apoptotic cells are marked by green fluorescence. The photographs shown were taken at identical exposure at ×400 magnification.

Table 1. RLIP protein concentrations and transport activity in melanoma and non-malignant cell lines

	Total crude protein	RLIP protein		Transport activity (pmol/min/mg)	
	mg/10^8 cells	µg/10^8 cells	% of total protein	^{14}C-DOX	^{3}H-DNP-SG
Human melanoma					
A101D	6.84 ± 0.54	42 ± 5	0.62	266 ± 24	878 ± 64
A2058	7.28 ± 0.92	57 ± 4	0.78	344 ± 32	1148 ± 102
A375	6.98 ± 0.72	64 ± 8	0.92	405 ± 34	1314 ± 94
G361	7.36 ± 0.82	65 ± 6	0.89	412 ± 28	1322 ± 86
MeWo	7.48 ± 0.66	63 ± 7	0.84	394 ± 26	1244 ± 114
SKMEL2	6.92 ± 0.58	63 ± 5	0.91	401 ± 36	1268 ± 76
SKMEL5	7.64 ± 0.84	66 ± 7	0.86	422 ± 44	1426 ± 128
SKMEL28	7.26 ± 0.62	61 ± 4	0.82	364 ± 38	1136 ± 92
Non-malignant					
NHDF	6.68 ± 0.78	12 ± 1	0.18	34 ± 4	102 ± 9
HAVSMC	6.24 ± 0.72	11 ± 1	0.17	38 ± 5	104 ± 12
HUVEC	6.82 ± 0.64	14 ± 1	0.21	34 ± 3	108 ± 11

Homogenate was prepared from 100 × 10^6 cultured cells. RLIP was quantified by ELISA. Purified recombinant RLIP was used to generate calibration curves. For transport studies, the plasma membrane fraction obtained from 2 × 10^7 cells was enriched for IOVs by wheat-germ agglutinin affinity chromatography (11,22). Transport activity was calculated based on measurements of the uptake of ^{14}C-DOX (specific activity 8.4 × 10^4 cpm/nmol) or ^{3}H-DNP-SG (specific activity 3.8 × 10^3 cpm/nmol) into IOVs (20 µg/30 µl reaction mixture) in the absence or presence of 4 mM ATP after 10 min incubation at 37°C, as previously described (11). Each transport study was performed with three replicates in three independent experiments (n = 9).

from normal cells. The ATP-dependent transport of both ^{14}C-DOX and ^{3}H-DNP-SG was greater in melanoma cells containing greater amounts of RLIP protein, and there was a general correlation between RLIP protein levels and transport activity (Table 1). Thus, greater RLIP expression corresponded to greater transport activity.

Relative contribution of RLIP toward DOX transport

DOX is a common allocrite transported by RLIP (11), MRP1 (27) and MDR1 (28). Therefore, we quantified the relative contributions of these transporters to the ATP-dependent transport of DOX in SKMEL2 melanoma cells using an immunological approach. We previously showed that anti-RLIP IgG inhibits DOX transport in IOVs (29). Likewise, antibodies against MRP and Pgp also inhibit transport activity in IOVs (30,31). Thus, we designed experiments to measure the ATP-dependent uptake of ^{14}C-DOX by IOVs prepared from SKMEL2 cells and coated with anti-RLIP IgG, anti-MRP1 IgG or anti-MDR1 IgG. The optimal concentrations to specifically inhibit DOX transport were determined in titration studies in which varying concentrations of each antibody were used to coat the membrane vesicles. Anti-RLIP IgG, which specifically recognized only RLIP in crude extracts of SKMEL2 cells, inhibited 65 ± 9% of total DOX transport in IOVs prepared from SKMEL2 cells. Anti-MRP IgG also inhibited DOX transport in a saturable manner, but the maximal inhibition achieved (26 ± 4%) was less than that of anti-RLIP IgG. Anti-Pgp IgG had a small but detectable inhibitory effect on DOX transport (5 ± 2%). This study also established that <40 µg/ml of each antibody was sufficient to quantitatively inhibited the transport activity of each respective antigen present in the amount of vesicles used (20 µg/30 µl reaction mixture). In vesicles coated with a mixture of all three antibodies, almost complete abrogation of DOX transport (91 ± 6%) was observed. In control vesicles coated with pre-immune IgG, transport activity remained unaffected. These results demonstrate that RLIP, MRP and Pgp together constitute nearly all ATP-dependent transport activity in these membranes. Furthermore, these results established that RLIP accounts for the majority (about two-thirds) of ATP-dependent DOX transport in melanoma cells.

RLIP inhibition and depletion cause preferential cytotoxicity in melanoma cells

The cytotoxic effects of RLIP inhibition by antibodies and RLIP depletion by antisense on melanoma cells were assessed using an established MTT assay (16). Cells were treated with pre-immune IgG, control scrambled antisense, anti-RLIP IgG (40 µg/ml) or RLIP antisense (20 µg/ml) for 48 h. Both RLIP-targeting agents exhibited preferential toxicity against melanoma cells compared to nonmalignant cells, consistent with our observations of other malignant (lung, colon, kidney and prostate) cell lines in similar experiments (16,32–35). Compared with their respective controls, RLIP IgG (Figure 2A) and RLIP antisense (Figure 2B) had significant growth inhibitory effects on melanoma cells. In contrast, RLIP inhibition and depletion did not have significant growth inhibitory effects on normal epithelial cells. Figure 2C shows the percentage of surviving cells in each cell line upon treatment with RLIP IgG or RLIP antisense. Figure 2D lists the genetic mutations present in the melanoma cell lines.

RLIP inhibition and depletion cause regression of melanoma xenografts in nude mice

The ultimate pre-clinical test of the potential utility of an anti-neoplastic agent is to demonstrate its effectiveness in an animal model. Thus, the anti-neoplastic effects of RLIP inhibition and depletion were examined in a xenograft model of melanoma. Mice bearing subcutaneous tumors (~33 mm^2) were treated with 5 mg/kg b.w. of RLIP antibodies, RLIP antisense, or their respective controls (pre-immune serum or control antisense) by intraperitoneal injection. The tumors of mice that received the RLIP-targeting agents exhibited rapid and dramatic reductions in size, whereas the tumors of mice in the control treatment groups showed uncontrolled growth. This remarkable difference in outcomes was clearly evident for melanoma cell lines (Figure 3 and Supplementary Figures 1 and 2, available at *Carcinogenesis* Online). The weight gain of the tumor-bearing mice was comparable to that of non-tumor-bearing controls, and no overt toxicity was evident among the mice tested (Figure 3A and D). A remarkable contrast in tumor growth was also clearly evident

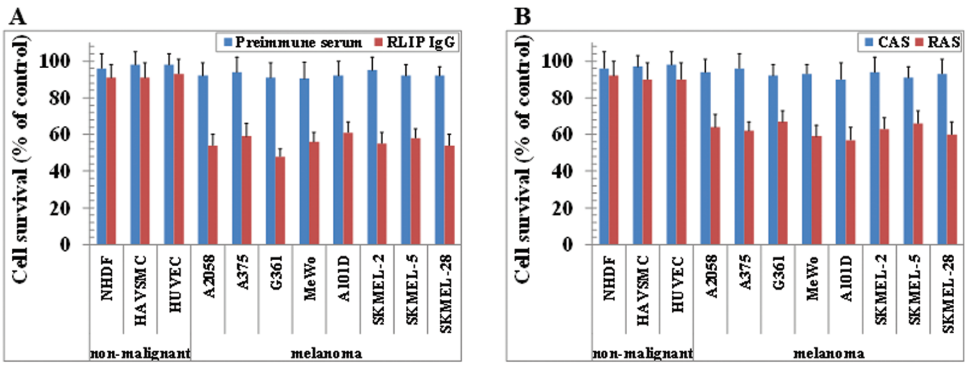

C

Cell Line	Cell survival 48 h post treatment (% of control)	
	RLIP antibodies (40 µg/ml conc.)	RLIP antisense (20 µg/ml conc.)
NHDF	91+7	92+8
HAVSMC	91±8	90±9
HUVEC	93±8	90±9
A2058	54±6	64±7
A375	59±7	62±5
G361	48±4	67±6
MeWo	56±5	59±6
A101D	61±6	57±7
SKMEL-2	55±6	63±6
SKMEL-5	58+5	66+7
SKMEL-28	54±6	60±7

D

Genetic mutation in melanoma cell lines

Melanoma cell lines	NRAS status	BRAF status	LKB1 status	p53 status	tumor formation
A2058	wild type	V599E	-ve	V274F	yes
A375	wild type	V600E	wild type	wild type	yes
G361	mutated	mutated	mutated		yes
MeWo	wild type	wild type	wild type	wild type	yes
A101D	wild type	V600E	wild type	wild type	
SKMEL-2	Q61R	wild type	wild type	G245S	yes
SKMEL-5	wild type	V600E	-ve	wild type	yes
SKMEL-28	wild type	V599E	wild type	wild type	yes

Figure 2. Effects of RLIP antibody and RLIP antisense on cell viability. Comparison of the cytotoxic effects of anti-RLIP IgG and RLIP antisense on melanoma versus normal cells. **(A)** The effect of pre-immune IgG (blue columns) and anti-RLIP IgG (red columns; 40 µg/ml final concentration) on cell survival was determined by MTT assays conducted 48 h after treatment. **(B)** MTT assays were also conducted 48 h after treatment with scrambled antisense (CAS, blue columns) and RLIP antisense (RAS, red columns; 20 µg/ml final concentration) using Maxfect transfection reagent. **(C)** The percentage of surviving cells in each cell line after treatment with RLIP antibodies and RLIP antisense. The data are presented as mean ± SD from three separate experiments with eight replicates each (n = 24). **(D)** Genetic mutations in each human melanoma cell line.

(Figure 3B and E). Compared with the control treatments, the RLIP-targeting agents caused a significant reduction in tumor weight. At the end of the study, on day 50 after the initiation of treatment, the average final tumor weights were significantly lower in both SKMEL2 (Figure 3C) and SKMEL5 (Figure 3F) xenograft-bearing mice that received RLIP-targeting agents compared to respective controls (Figure 3C—SKMEL2 melanoma tumor xenograft model: pre-immune serum, 1.82 g; scrambled antisense, 1.98 g; versus RLIP antibody, 0.64 g; RLIP antisense, 0.53 g; Figure 3F—SKMEL5 melanoma tumor xenograft model: pre-immune serum, 1.68 g; scrambled antisense, 1.84 g; versus RLIP antibody, 0.58 g, RLIP antisense, 0.51 g). No macroscopic evidence of metastasis to other organs was evident for any experimental groups. These studies demonstrate the significant and sustained regression of SKMEL2 and SKMEL5 xenografts upon targeted depletion of the MAP transporter protein RLIP.

Protein levels in tumor tissue after RLIP antisense treatment

The constitutive activation of signal transducer and activator of transcription 3 (STAT3), mediated by Src and Janus kinase (JAK) tyrosine kinases, participates in the regulation of tumor cell growth (36,37). The function of JAKs has been associated with the activation of the STAT signaling pathway (38). The activation of STAT3 signaling has an important role in melanoma oncogenesis (39). Tumor tissue lysates from mice treated with control scrambled antisense or RLIP antisense were assessed by western blot and immunohistochemistry for the expression of proliferation, apoptosis and cell cycle markers. Western blot analysis showed that, compared with the control treatment, treatment with RLIP antisense reduced the protein expression of RLIP and the cell cycle regulatory proteins CDK4 and cyclin B1; inhibited the phosphorylation (activation) of STAT3, JAK2 and Src, as well as the expression of Mcl-1 and Bcl2; and increased levels of Bax and pAMPK (Figure 4). Taken together, these data suggest that RLIP antisense inhibits the JAK2/STAT3 signaling pathway in melanoma cells, leading to the induction of apoptosis.

Impact of RLIP depletion on markers of tumor cell proliferation and angiogenesis

Upon completion of the *in vivo* studies, paraffin-embedded xenograft tumor sections were histopathologically examined by hematoxylin and eosin staining. This examination revealed that RLIP depletion by antisense, but not the control treatment, reduced the number of tumor blood vessels and restored normal morphology. Avidin/biotin complex staining revealed that RLIP antisense treatment also reduced levels of the proliferation markers RLIP and Ki67, as well as the angiogenesis marker CD31. AMPK is a critical cellular protein that senses the low energy status of cells and inhibits cell proliferation and survival (40). RLIP depletion increased levels of pAMPK in tumor sections, providing corroborative evidence for the anti-tumor effects of RLIP antisense in *in vivo* models of melanoma (Figure 5). Taken together, our results indicate that RLIP antisense displays strong anticancer effects in melanoma.

As existing therapies do not greatly improve the survival rates of patients with advanced melanoma, it is critical to find new treatments based on a better understanding of the molecular mechanisms underlying its malignant progression. In our study, RLIP antisense induced apoptosis in melanoma cells both *in vitro*

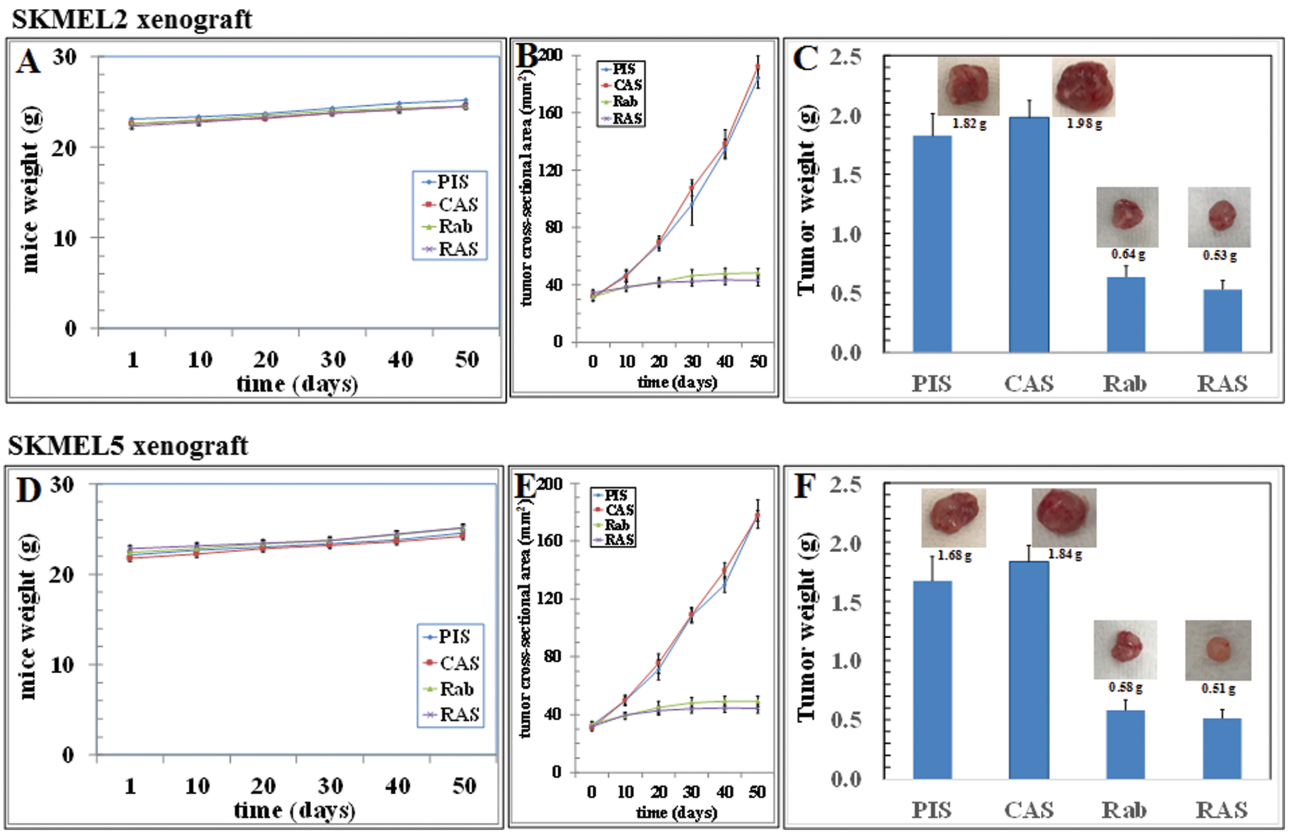

Figure 3. Effects of RLIP-targeting agents on tumor growth. Athymic nude mice were implanted with SKMEL2 and SKMEL5 human melanoma cells and treated with 5 mg/kg b.w. of pre-immune serum (PIS), RLIP antibody (Rab), control scrambled antisense (CAS) or RLIP antisense (RAS). Weight gain **(A, D)**, tumor cross-sectional area **(B, E)** and tumor weight **(C, F)** were determined for each treatment group at the end of the study (day 50). Each value in the line and bar graphs represents the mean ± SD from five mice in each group. Photographs of the tumors were also taken on day 50.

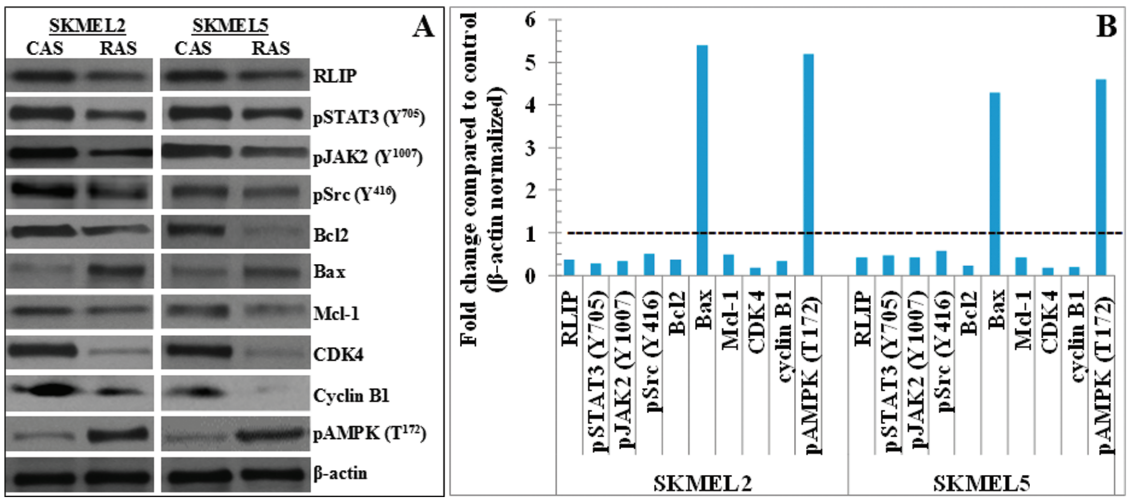

Figure 4. Effects of RLIP antisense on the expression of various proteins in tumor tissues. **(A)** Tumor tissue excised from SKMEL2 and SKMEL5 xenograft-bearing mice treated with control scrambled (CAS) or RLIP antisense (RAS) were analyzed for changes in expression levels of RLIP, pSTAT3 (Y^{705}), pJAK2 (Y^{1007}), pSrc (Y^{416}), Bcl2, Bax, Mcl-1, CDK4, cyclin B1 and pAMPK (T^{172}). β-Actin was used as a loading control. **(B)** Bar diagram showing the quantification of protein expression based on the Western blots shown in **(A)**. The dotted lines indicate the protein expression levels in control tissues.

and *in vivo*. Furthermore, we found that the anti-tumor activity of RLIP antisense is associated with the downregulation of JAK2/STAT3 signaling in melanoma cells, suggesting that the inhibition of the JAK/STAT3 pathway could be a potential therapeutic approach for melanoma. Our study also revealed that RLIP antisense reduced the tyrosine phosphorylation of STAT3 *in vivo*, and this suppression was mediated by a reduction in the phosphorylation of JAK2. Therefore, targeting STAT3 may be a promising therapeutic strategy to prevent or inhibit metastasis in melanoma patients and warrants further clinical investigation.

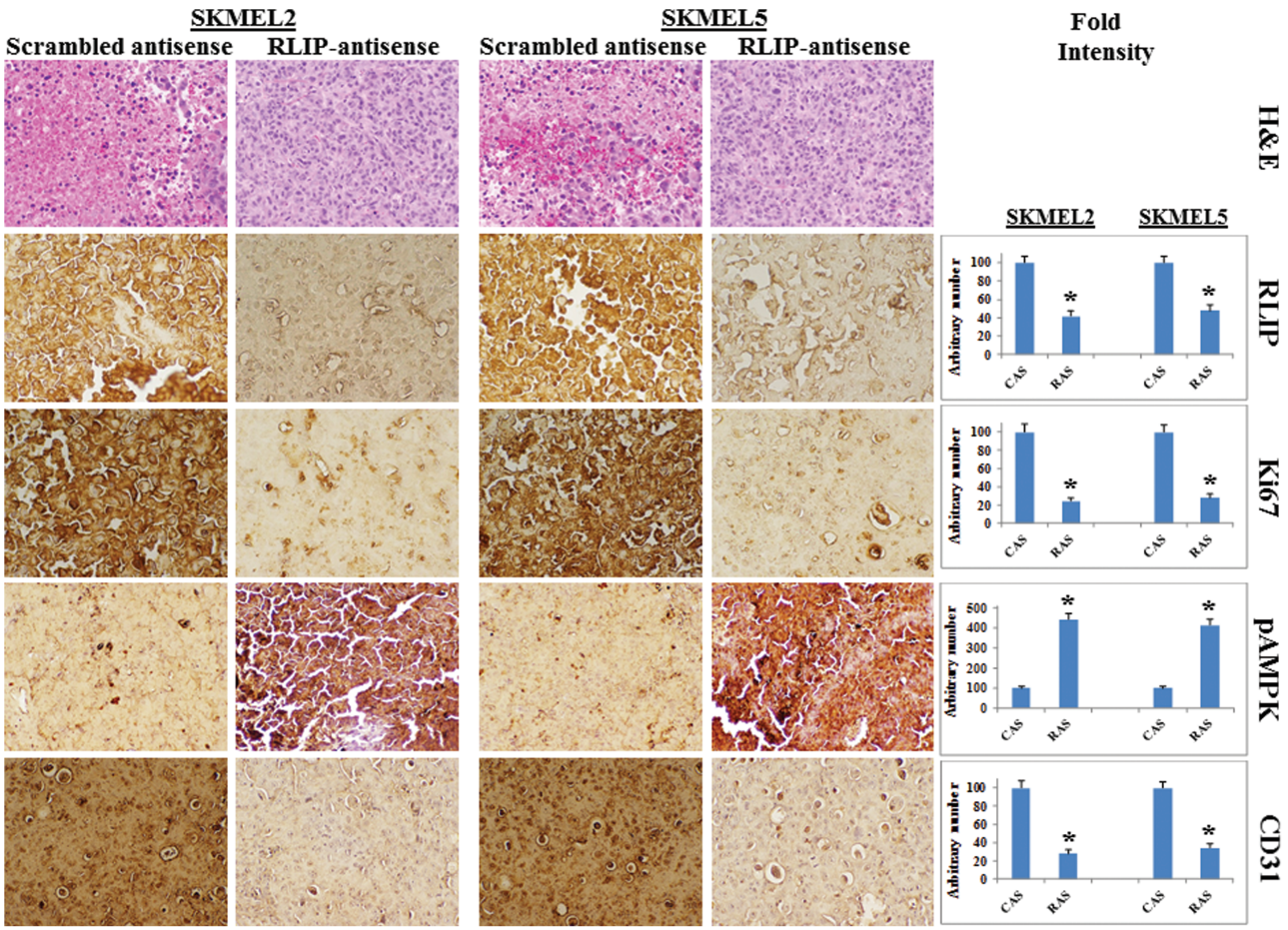

Figure 5. Immunohistochemical analysis of proliferation and angiogenesis markers in SKMEL2 and SKMEL5 xenograft tumors. Immunohistochemical analysis was conducted using tumor tissues from SKMEL2 and SKMEL5 xenograft-bearing mice treated with control scrambled (CAS) and RLIP antisense (RAS). Hematoxylin and eosin staining and staining to detect RLIP, Ki67, pAMPK and CD31 were performed. Photomicrographs at ×40 magnification were acquired using an Olympus DP 72 microscope. The percentage of stained tissue was determined by measuring positive immunoreactivity per unit area. The intensity of antigen staining was quantified by digital image analysis using Pro Plus software. One representative image for each treatment group is shown. Bars represent mean ± SE ($n = 5$). The statistical significance of differences between groups was determined by two-tailed Student's *t*-test. *$P < 0.01$, compared with controls.

Discussion

STAT proteins play an important role in oncogenic signaling (36,37). The constitutive activation of STATs, including STAT3 and STAT5, is frequently observed in human tumor cells and tissues. STATs have essential functions in regulating cell proliferation, differentiation, survival, angiogenesis and immune function. One of the seven different STAT family members, STAT3, is persistently activated by non-receptor tyrosine kinases, such as JAKs or Src family kinases (37). The constitutive activation of STAT3 has a critical role in cell growth and survival in human solid tumor malignancies. STAT3 activation requires Tyr^{705} phosphorylation, resulting in dimerization, nuclear translocation, DNA binding and transcriptional activation of target genes, such as Mcl-1, survivin, Bcl-2 and cyclin D1 (41). STAT3 regulates basic biologic processes important in tumorigenesis, including cell cycle progression, survival, tumor angiogenesis and tumor cell evasion of the immune system (37). Many of the studies that defined the role of STAT3 in oncogenesis were carried out in cancer cells and animal models of melanoma, and targeting STAT3 signaling in melanoma cells is an appealing strategy (39). In STAT3 signaling, two phosphorylated STAT3 monomers dimerize through reciprocal phosphotyrosyl-SH2 domain interactions. The phosphorylated STAT3 dimers then translocate to the nucleus and bind to the promoters of specific STAT3-responsive genes. Constitutively activated STAT3 upregulates the expression of the anti-apoptotic proteins Mcl-1 and Bcl2 in human cancer cells (36). In contrast, the blockade of STAT3 signaling downregulates these downstream target genes associated with the induction of apoptosis in human cancer cells.

Proteins in the JAK family, including JAK1, JAK2, JAK3 and tyrosine kinase 2 (Tyk2), display similar structures and functions. JAKs are activated by interferons and growth hormones. The activation of JAKs is critical in cytokine receptor signaling. Constitutively activated JAKs phosphorylate critical cellular substrates associated with oncogenic signaling pathways, such as STAT family members, including STAT3. Activated JAK/STAT signaling has been extensively validated as a targetable molecular pathway for treating solid tumors (36–38).

Malignant melanoma is a neoplasm of melanocytic cells with rising incidence. Although most cases are identified early, even early-stage malignant melanoma can metastasize. The lymph nodes are often the initial sites of metastasis, but distant metastases also occur and are almost uniformly fatal (1–3). Using current standard clinical measures, there is limited ability to predict, detect and prevent lymph node and distal metastases

in patients with the propensity to develop them. This calls for new biomarkers and preventive strategies.

RLIP is the gene product of *RALBP1*, located at chromosome 18p11.22. RLIP is a central regulator of cellular oxidative stress and is pivotal for the export of electrophilic and non-electrophilic xenobiotics, including chemotherapeutic agents and targeted therapies (11–14). RLIP also has a central role in intracellular signal transduction processes, binding to multiple proteins, such as Ral A and B, Hsf1, AP2, ARIP2 (activin receptor-interacting protein-2), POB1, CDK1, PKCα and cdc42. It has been shown to function as an effector protein for RalA and RalB, mediating GTPase-activating protein activity for cdc42 and Rac1 (11–13,42). In several pre-clinical models, as well as clinical studies, RLIP has been shown to correlate with the metastatic potential of various neoplasms (23–25,42–45). In addition, we have shown that RLIP knockout completely abrogates CDE (46).

The success of any targeted therapy to treat human malignancies relies on its ability to demonstrate potential in multiple stages of drug development. In this regard, RLIP antisense has tremendous advantages as a potential treatment for melanoma, as demonstrated by established scientific evidence. RLIP antisense has been extensively tested in several cancers, including cancers of the lung, breast, colon, kidney and prostate, as well as neuroblastoma (32–35,47,48). In these past studies, antisense-induced depletion of RLIP specifically targeted tumor cells while sparing normal cells. In extensive animal experiments, RLIP antisense effectively induced tumor regression without causing any overt toxicity to normal organ tissues that could compromise function. The most remarkable side effects of RLIP depletion were moderate hypoglycemia and hypolipidemia, which are both considered salutary in humans. Most importantly, mice treated with RLIP antisense and $RLIP^{-/-}$ mice are developmentally normal, exhibiting normal weight gain without any deficits in activity (49–52). Thus, in addition to a strong mechanistic rationale supporting the development of RLIP antisense as a safe, effective and innovative therapeutic intervention for melanoma, further investigations into this approach are supported by a plethora of characteristics desirable an ideal anticancer drug.

In summary, our findings demonstrate that RLIP antisense inhibits JAK2 phosphorylation, resulting in the inhibition of constitutively activated STAT3 signaling. RLIP depletion in human melanoma cells induces apoptosis associated with the downregulation of Mcl-1 and Bcl2, two gene products downstream of STAT3. These results suggest that the anti-tumor activity of RLIP antisense is at least partially caused by the inhibition of JAK2/STAT3 signaling in human melanoma cells. Thus, these findings suggest a pharmacological mechanism of action of RLIP antisense in human cancer cells that has important implications for solid tumor treatment. In particular, RLIP antisense represents a promising lead compound for the development of new therapeutics for cancer treatment.

Significance

Currently, there are limited treatment options for malignant melanoma and no effective chemotherapeutic strategies that are safe, affordable and effective. The most innovative aspect of the current study is the use of rational and melanoma signaling-specific experiments to investigate the mechanisms consequent to targeting RLIP with safe and well-characterized RLIP antisense and RLIP antibodies. The clinical development of these agents is supported by strong preliminary evidence showing their strong anti-tumor effects against melanoma, while sparing normal cells, in both *in vitro* cell culture and *in vivo* mouse melanoma model studies. This systematic investigation into the melanoma-specific anticancer effects of RLIP depletion/inhibition will expand our understanding of the critical signaling nodes that regulate melanocyte transformation, survival and progression. In addition, this work has characterized and validated the use of RLIP-targeting agents as a novel therapeutic approach to effectively control human malignant melanoma.

Conclusions

Melanoma is the sixth most common malignancy in the United States, and its rate of incidence is increasing. Fair-skinned and young individuals are at higher risker for developing melanoma. Of particular concern is the finding that individuals diagnosed with malignant skin lesions are relatively young, with a median age of 42 years (range = 24–57 years). Current treatment options for advanced melanoma are not curative, and the 5-year mortality rate is 85%. Hence, the development of novel targeted therapies has assumed immense significance in translational melanoma research. In this regard, the novel RLIP antisense has demonstrated potent anti-melanoma activity both *in vitro* and *in vivo*, and the RLIP antisense-induced apoptosis of human melanoma cells was associated with reduced phosphorylation of JAKs and STAT3. Consistent with the inhibition of STAT3 signaling, the expression of the anti-apoptotic protein Mcl-1 was downregulated. Hence, the further characterization and validation of the mechanistic basis of the anti-melanoma effects of RLIP antisense represent a promising avenue in melanoma drug development. The results of this study provide a sound scientific rationale for the development of new dosage formulations and clinical trials to evaluate the use of RLIP antisense to control human malignant melanoma. These future studies may, in turn, lead to new therapies that may be effective for patients whose melanoma has become refractory to current therapies, ultimately reducing the suffering caused by this disease.

Highlights

- RLIP antisense treatment reduced levels of RLIP, pSTAT3, pJAK2, pSrc, Mcl-1 and Bcl2, as well as CDK4 and cyclin B1, and increased levels of Bax and pAMPK.
- Compounds that inhibit, deplete or downregulate RLIP will function as wide-spectrum agents to treat melanoma, independent of common signaling pathway mutations.
- This work has characterized and validated the use of RLIP-targeting agents as a novel therapeutic approach to effectively control human malignant melanoma.
- Overall, RLIP plays an essential role in melanoma progression.

Funding

This work was supported in part by grants from the United States Department of Defense (W81XWH-16-1-0641 and W81XWH-20-1-0362) and the National Cancer Institute of the National Institutes of Health (P30CA33572). Funding from the Beckman Research Institute of City of Hope is also acknowledged.

Acknowledgements

We thank the personnel in the Animal Research Center and Pathology Cores for their invaluable assistance. We sincerely thank Dr. Ravi Salgia, MD, PhD, Professor and Chair, Department of Medical Oncology at City of Hope, for providing research space and support. No human subjects were involved in the

present study. All animal studies were conducted according to a protocol approved by the City of Hope Animal Care and Ethics Committee (IACUC protocol # 20033). All data generated and analyzed during the current study are available from the corresponding author upon request.

Author contributions

Sharad S. Singhal contributed to data collection and wrote the manuscript. Atish Mohanty contributed to analysis and interpretation of data. Prakash Kulkarni contributed to literature search and statistical analysis. David Horne contributed to reviewing/editing the manuscript. Sanjay Awasthi contributed to discussion and review/editing the manuscript. Ravi Salgia contributed to data interpretation

Conflict of Interest Statement: None declared.

References

1. Rebecca, V.W. *et al.* (2020) Pre-clinical modeling of cutaneous melanoma. *Nat. Commun.*, 11, 2858.
2. Jenkins, R.W. *et al.* (2021) Treatment of advanced melanoma in 2020 and beyond. *J. Invest. Dermatol.*, 141, 23–31.
3. Robert, C. *et al.* (2011) Ipilimumab plus dacarbazine for previously untreated metastatic melanoma. *N. Engl. J. Med.*, 364, 2517–2526.
4. Smalley, K.S. *et al.* (2009) Integrating BRAF/MEK inhibitors into combination therapy for melanoma. *Br. J. Cancer*, 100, 431–435.
5. Solit, D.B. *et al.* (2006) BRAF mutation predicts sensitivity to MEK inhibition. *Nature*, 439, 358–362.
6. Smalley, K.S. *et al.* (2008) Increased cyclin D1 expression can mediate BRAF inhibitor resistance in BRAF V600E-mutated melanomas. *Mol. Cancer Ther.*, 7, 2876–2883.
7. Grant, S. *et al.* (2007) Co-targeting survival signaling pathways in cancer. *J. Clin. Invest.*, 118, 3003–3006.
8. Modok, S. *et al.* (2006) Modulation of multidrug resistance efflux pump activity to overcome chemoresistance in cancer. *Curr. Opin. Pharmacol.*, 6, 350–354.
9. Robey, R.W. *et al.* (2008) Inhibition of P-glycoprotein (ABCB1)- and multidrug resistance-associated protein 1 (ABCC1)-mediated transport by the orally administered inhibitor, CBT-1®. *Biochem. Pharmacol.*, 75, 1302–1312.
10. Shukla, S. *et al.* (2008) Development of inhibitors of ATP-binding cassette drug transporters: present status and challenges. *Expert Opin. Drug Metab. Toxicol.*, 4, 205–223.
11. Awasthi, S. *et al.* (2000) Novel function of human RLIP76: ATP-dependent transport of glutathione conjugates and doxorubicin. *Biochemistry*, 39, 9327–9334.
12. Awasthi, S. *et al.* (2003) Transport of glutathione conjugates and chemotherapeutic drugs by RLIP76 (RALBP1): a novel link between G-protein and tyrosine kinase signaling and drug resistance. *Int. J. Cancer*, 106, 635–646.
13. Awasthi, S. *et al.* (2008) RLIP76 and Cancer. *Clin. Cancer Res.*, 14, 4372–4377.
14. Singhal, J. *et al.* (2008) RLIP76 in defense of radiation poisoning. *Int. J. Radiat. Oncol. Biol. Phys.*, 72, 553–561.
15. Schadendorf, D. *et al.* (1995) Glutathione and related enzymes in tumor progression and metastases of human melanoma. *J. Invest. Dermatol.*, 105, 109–112.
16. Singhal, S.S. *et al.* (2006) Regression of melanoma in a murine model by RLIP76 depletion. *Cancer Res.*, 66, 2354–2360.
17. Liu, L. *et al.* (2011) 6-Bromoindirubin-3′-oxime inhibits JAK/STAT3 signaling and induces apoptosis of human melanoma cells. *Cancer Res.*, 71, 3972–3979.
18. Ma, D.L. *et al.* (2014) Virtual screening and optimization of Type II inhibitors of JAK2 from a natural product library. *Chem. Commun. (Camb).*, 50, 13885–13888.
19. Tian, Y. *et al.* (2012) Spirooxindole derivative SOID-8 induces apoptosis associated with inhibition of JAK2/STAT3 signaling in melanoma cells. *PLoS One*, 7, e49306.
20. Bild, A.H. *et al.* (2002) Cytoplasmic transport of Stat3 by receptor-mediated endocytosis. *EMBO J.*, 21, 3255–3263.
21. Awasthi, Y.C. *et al.* (1981) Enzymatic conjugation of erythrocyte glutathione with 1-chloro-2,4-dinitrobenzene: the fate of glutathione conjugate in erythrocytes and the effect of glutathione depletion on hemoglobin. *Blood*, 58, 733–738.
22. Awasthi, S. *et al.* (1994) Adenosine-triphosphate-dependent transport of doxorubicin, daunomyicn, and vinblastine in human tissues by a mechanism distinct from the P-glycoprotein. *J. Clin. Invest.*, 93, 958–965.
23. Wang, Q. *et al.* (2013) RLIP76 is overexpressed in human glioblastomas and is required for proliferation, tumorigenesis and suppression of apoptosis. *Carcinogenesis*, 34, 916–926.
24. Zhong, W. *et al.* (2010) RalBP1 is necessary for metastasis of human cancer cell lines. *Neoplasia*, 12, 1003–1012.
25. Wang, C.Z. *et al.* (2015) RLIP76 expression as a prognostic marker of breast cancer. *Eur. Rev. Med. Pharmacol. Sci.*, 19, 2105–2111.
26. Sharma, R. *et al.* (2004) RLIP76-mediated transport of leukotriene C4 in cancer cells: implications in drug-resistance. *Int. J. Cancer*, 112, 934–942.
27. Lautier, D. *et al.* (1996) Multidrug-resistance mediated by the multidrug-resistance protein (MRP) gene. *Biochem. Pharmacol.*, 52, 967–977.
28. Gottesman, M.M. *et al.* (1993) Biochemistry of multidrug-resistance mediated by the multidrug-transporter. *Annu. Rev. Biochem.*, 62, 385–427.
29. Awasthi, S. *et al.* (2003) Role of RLIP76 in lung cancer doxorubicin-resistance: Doxorubicin-transport in lung cancer by RLIP76. *Int. J. Oncol.*, 22, 713–720.
30. Hipfner, D.R. *et al.* (1999) Monoclonal-antibodies that inhibit the transport function of the 190-kDa multidrug-resistance protein, MRP. Localization of their epitopes to the nucleotide-binding-domains of the protein. *J. Biol. Chem.*, 274, 15420–15426.
31. Kokubu, N. *et al.* (1997) Functional modulation of ATPase of P-glycoprotein by C219, a monoclonal-antibody against P-glycoprotein. *Biochem. Biophys. Res. Commun.*, 230, 398–401.
32. Singhal, S.S. *et al.* (2007) Regression of lung and colon cancer xenografts by depleting or inhibiting RLIP76 (Ral-binding protein 1). *Cancer Res.*, 67, 4382–4389.
33. Singhal, S.S. *et al.* (2009) Regression of prostate cancer xenografts by RLIP76 depletion. *Biochem. Pharmacol.*, 77, 1074–1083.
34. Singhal, S.S. *et al.* (2009) RLIP76: a target for kidney cancer therapy. *Cancer Res.*, 69, 4244–4251.
35. Singhal, J. *et al.* (2011) Targeting p53 null neuroblastomas through RLIP76. *Cancer Prev. Res.*, 4, 879–889.
36. Yu, H. *et al.* (2004) The STATs of cancer – new molecular targets come of age. *Nat. Rev. Cancer*, 4, 97–105.
37. Yu, H. *et al.* (2009) STATs in cancer inflammation and immunity: a leading role for STAT3. *Nat. Rev. Cancer*, 9, 798–809.
38. Reddy, E.P. *et al.* (2000) IL-3 signaling and the role of Src kinases, JAKs and STATs: a covert liaison unveiled. *Oncogene*, 19, 2532–2547.
39. Kortylewski, M. *et al.* (2005) Targeting STAT3 affects melanoma on multiple fronts. *Cancer Metastasis Rev.*, 24, 315–327.
40. Woodard, J. *et al.* (2010) AMP-activated kinase (AMPK)-generated signals in malignant melanoma cell growth and survival. *Biochem. Biophys. Res. Commun.*, 398, 135–139.
41. Gritsko, T. *et al.* (2006) Persistent activation of stat3 signaling induces survivin gene expression and confers resistance to apoptosis in human breast cancer cells. *Clin. Cancer Res.*, 12, 11–19.
42. Neel, N.F. *et al.* (2012) The RalB small GTPase mediates formation of invadopodia through a GTPase-activating protein-independent function of the RalBP1/RLIP76 effector. *Mol. Cell. Biol.*, 32, 1374–1386.
43. Rybko, V.A. *et al.* (2011) Different metastasis promotive potency of small G-proteins RalA and RalB in *in vivo* hamster tumor model. *Cancer Cell Int.*, 11, 22.
44. Mollberg, N.M. *et al.* (2012) Overexpression of RalBP1 in colorectal cancer is an independent predictor of poor survival and early tumor relapse. *Cancer Biol. Ther.*, 13, 694–700.
45. Lee, S. *et al.* (2012) RALBP1/RLIP76 depletion in mice suppresses tumor growth by inhibiting tumor neovascularization. *Cancer Res.*, 72, 5165–5173.
46. Singhal, S.S. *et al.* (2011) Glutathione-conjugate transport by RLIP76 is required for clathrin-dependent endocytosis and chemical carcinogenesis. *Mol. Cancer Ther.*, 10, 16–28.

47. Singhal, *J. et al.* (2018) 2′-Hydroxyflavanone inhibits *in vitro* and *in vivo* growth of breast cancer cells by targeting RLIP76. *Mol. Carcinog.*, 57, 1751–1762.
48. Singhal, *J. et al.* (2019) RLIP inhibition suppresses breast-to-lung metastasis. *Cancer Lett.*, 447, 24–32.
49. Awasthi, S. *et al.* (2005) RLIP76 is a major determinant of radiation sensitivity. *Cancer Res.*, 65, 6022–6028.
50. Bose, C. *et al.* (2019) Topical 2′-hydroxyflavanone for cutaneous melanoma. *Cancers*, 11, 1556.
51. Singhal, S.S. *et al.* (2020) RLIP controls receptor-ligand signaling by regulating clathrin-dependent endocytosis. *Biochim. Biophys. Acta. Rev. Cancer*, 1873, 188337.
52. Singhal, *J. et al.* (2021) Targeting RLIP with CRISPR/Cas9 controls tumor growth. *Carcinogenesis*, 42, 48–57.